European Heart Journal Supplements (2022) **24** (Supplement C), C233–C242
The Heart of the Matter
https://doi.org/10.1093/eurheartj/suac014

Update on supra-annular sizing of transcatheter aortic valve prostheses in raphe-type bicuspid aortic valve disease according to the LIRA method

Gianmarco Iannopollo[1,2*†], Vittorio Romano[1†], Antonio Esposito[3,4], Giulia Guazzoni[1], Marco Ancona[1], Luca Ferri[1], Filippo Russo[1], Barbara Bellini[1], Nicola Buzzatti[1,5], Jonathan Curio[6], Bernard Prendergast[7], and Matteo Montorfano[1]

[1]*Interventional Cardiology Unit, San Raffaele Scientific Institute, Via Olgettina 60, Milan 20132, Italy*
[2]*Department of Cardiology, Maggiore Hospital Carlo Alberto Pizzardi, Bologna, Italy*
[3]*Experimental Imaging Centre, Radiology Unit, IRCCS San Raffaele Scientific Institute, Milan, Italy*
[4]*School of Medicine, Vita-Salute San Raffaele University, Via Olgettina 58, Milan, Italy*
[5]*Cardiac Surgery Department, San Raffaele Scientific Institute, Via Olgettina 60, Milan 20132, Italy*
[6]*Department of Cardiology, Charité University Medical Care, Campus Benjamin Franklin, Berlin, Germany*
[7]*Department of Cardiology, St Thomas' Hospital, Cleveland Clinic London, London, UK*

KEYWORDS
bicuspid aortic valve disease;
TAVR;
MDCT;
TAVR prostheses sizing;
LIRA method

Recent evidence has shown that transcatheter heart valve (THV) anchoring in bicuspid aortic valve (BAV) patients occurs at the level of the raphe, known as the LIRA (Level of Implantation at the RAphe) plane. Our previous work in a cohort of 20 patients has shown that the delineation of the perimeter and device sizing at this level is associated with optimal procedural outcome. The goals of this study were to confirm the feasibility of this method, evaluate 30-day outcomes of LIRA sizing in a larger cohort of patients, assess interobserver variation and reproducibility of this sizing methodology, and analyse the interaction of LIRA-sized prostheses with the surrounding anatomy. The LIRA sizing method was applied to consecutive patients presenting to our centre with raphe-type BAV disease between November 2018 and October 2021. Supra-annular self-expanding THVs were sized based on baseline CT scan perimeters at the LIRA plane and the virtual basal ring. In cases where there was discrepancy between the two measurements, the plane with the smallest perimeter was considered the reference for prosthesis sizing. Post-procedural device success, defined according to Valve Academic Research Consortium-2 (VARC-2) criteria, was evaluated in the overall cohort. A total of 50 patients (mean age 80 ± 6 years, 70% male) with raphe-type BAV disease underwent transcatheter aortic valve replacement (TAVR) using different THV prostheses. The LIRA plane method appeared to be highly successful (100% VARC-2 device success) with no procedural mortality, no valve migration, no moderate-severe paravalvular leak, and low transprosthetic gradients (residual mean gradient 8.2 ± 3.4 mmHg). There were no strokes, no in-hospital or 30-day mortality, and an incidence of in-hospital pacemaker implantation of 10%. Furthermore, measurement of the LIRA plane perimeter was highly

*Corresponding author. Tel: +39 022 643 7331, Fax: +39 022 643 7339,
Email: gianmarco.iannopollo@libero.it
†The first two authors contributed equally to the study.

reproducible between observers ($r = 0.980$; $P < 0.001$) and predictive of the post-procedural prosthetic valve perimeter on CT scanning ($r = 0.981$; $P < 0.001$). We confirm the feasibility of supra-annular sizing using the LIRA method in a large cohort of patients with high procedural success and good clinical outcomes at 30 days. Application of the LIRA method optimizes THV prosthesis sizing in patients with raphe-type BAV disease.

Introduction

Transcatheter aortic valve replacement (TAVR) indications are expanding towards low surgical risk and younger patients with constant improvements in clinical outcomes.[1-3] In this cohort, the prevalence of bicuspid aortic valve (BAV) anatomy is expected to be higher.[4,5] Furthermore, octogenarians and nonagenarians account for 5–28% of the BAV population[6] and this cohort are likely to be referred for TAVR due to a higher risk of surgical complications related to age, frailty, and other comorbidities. Transcatheter aortic valve replacement in patients with BAV still represents a challenge due to the peculiar anatomy and lack of consensus concerning the optimal method for multi-detector computed tomography (MDCT) scan sizing and prosthesis selection.[7] Success rates have improved with the introduction of new-generation transcatheter heart valves (THVs),[8,9] although higher rates of procedural complications and clinical events persist in the BAV cohort,[10] especially in anatomical configurations combining a calcific raphe with excessive leaflet calcification.[11] Appropriate THV sizing is essential to optimize the interaction between the prosthesis and individual patient anatomy. Recent evidence has shown that THV anchoring in BAV patients occurs at the level of the raphe, also known as the LIRA (Level of Implantation at the RAphe) plane.[12] We have previously shown that the use of a novel supra-annular sizing method based on measurement of the perimeter at the level of the raphe (LIRA method) was safe and effective in a cohort of 20 BAV patients with severe aortic stenosis.[13] The goals of this study were to confirm the feasibility and clinical outcomes of LIRA sizing in a larger cohort of patients, assess interobserver reproducibility of this methodology, and analyse the interaction of LIRA-sized prostheses with the surrounding anatomy.

Methods

Study population

The LIRA sizing method was applied prospectively in all consecutive patients with aortic stenosis and raphe-type BAV disease treated with TAVR using a variety of supra-annular self-expandable prostheses at our centre between November 2018 and October 2021. Bicuspid aortic valve was defined as a deformed aortic valve with two functional cusps forming a valve mechanism with <3 zones of parallel apposition. The LIRA sizing method was applied to BAV Types 1 and 2 according to Sievers classification (Type 1—one raphe, Type 2—two raphes).[14] The diagnosis of BAV was confirmed by the local heart team based upon a review of the medical records, multi-detector CT scans, and transthoracic/transoesophageal echocardiography analysis when available. Patients were scheduled for TAVR following multidisciplinary discussion as indicated by current recommendations.[15] Post-procedural CT scans were performed according to local clinical protocols.

MDCT assessment

All subjects underwent electrocardiography-gated cardiac CT scanning before their TAVR procedure. All exams were independently analysed by one radiology technician and two cardiologists (V.R., G.I., and M.M.) using the Osirix programme, version 9 (Pixmeo SARL, Bernex, Switzerland, 2018). Computed tomography scans were analysed in systole (20–40% R-R interval) and the aortic valve virtual basal ring (VBR) defined as the short-axis plane through the nadir of each coronary cusp. The minimal diameter (D_{min}), maximal diameter (D_{max}), perimeter, and the area of the aortic valve VBR were determined (*Figure 1A*).

LIRA plane

The level of the aortic root where prosthesis anchoring was expected to occur (known as the LIRA plane) was identified on the pre-TAVR CT scan. The LIRA plane comprises the most rigid anatomical structures in the aortic root (calcific/fibrotic raphes) that might facilitate THV anchoring during deployment. In BAV Type 1 anatomy, the prosthesis should anchor at the level of the calcific/fibrotic raphe, whereas in BAV Type 2 anatomy presents two raphes and the THV prosthesis should anchor at the level of the major raphe (defined as that with the larger width and length, and greater amount of calcium). In both instances, the LIRA plane was identified as the level cutting the major raphe at its point of maximum protrusion along the aortic root (*Figure 1B and C*).[12]

LIRA sizing method

The LIRA plane represents a 'neo-VBR' where the perimeter traces the internal border of the leaflets, excluding all other structures encountered at this level (fused commissures, heavy calcification, and calcific or fibrotic raphes) (*Figure 1B*).[13] Transcatheter heart valves were sized according to manufacturer recommendations based on baseline CT scan perimeters at the VBR and LIRA plane. If there was a discrepancy in measurements between the two planes, the THV was sized according to the smallest perimeter. Transcatheter heart valve oversizing at the VBR and LIRA plane was expressed according to the cover index [100 − (prosthesis diameter − MDCT annular size)/

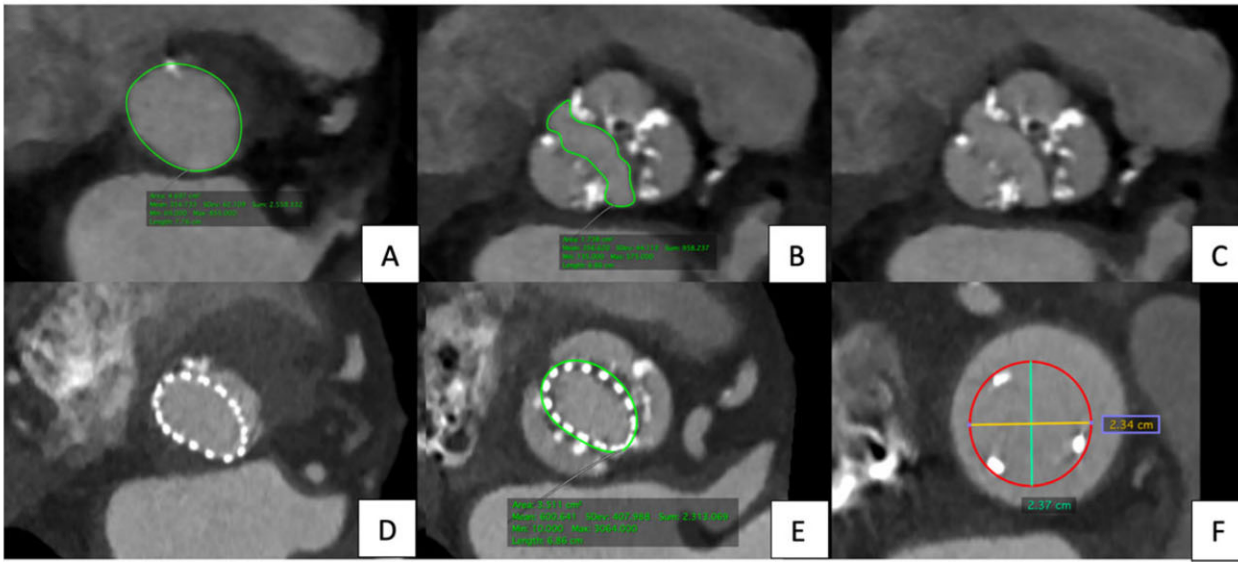

Figure 1 Prosthesis sizing according to the LIRA method. (*A*) Virtual basal ring measurements. (*B*) LIRA plane measurements. (*C*) LIRA plane level. (*D*) Transcatheter heart valve at virtual basal ring. (*E*) Transcatheter heart valve at the LIRA plane. (*F*) Transcatheter heart valve at coaptation level. LIRA, Level of Implantation at the RAphe.

prosthesis diameter][16] and the ratio between the implanted and expected THV diameter, according to VBR and LIRA plane measurements. We also evaluated the distance between the LIRA plane and VBR, the raphe length and its characteristics, and the ICD at a point 4 mm above the VBR (a previously established reference for THV sizing in BAV disease).[17]

Post-procedural MDCT assessment

Where available we evaluated post-TAVR CT scans to determine the interaction of the THV with surrounding anatomy. Specifically, we evaluated the perimeter of the THV at the LIRA plane, its distance from the VBR wall and the leaflets at the LIRA plane, and investigated the level of THV circularity at the VBR, LIRA plane, and coaptation level. Circularity was expressed as the eccentricity index [$EI = 1 - (D_{min}/D_{max})$].[18] Implantation depth was measured as the mean distance of the ventricular edge of the prostheses from the non-coronary cusp and the left coronary cusp of the native aortic valve.[19]

Study endpoints

The primary endpoint of the study was post-procedural device success, defined according to VARC-2 criteria. Secondary endpoints included in-hospital and 30-day outcomes. The severity of paravalvular leak (PVL) was qualitatively assessed and graded using transthoracic echocardiography.[20] To assess the reproducibility of measurements, we evaluated interobserver correlation of the LIRA plane perimeter. Correlation of pre- and post-procedural LIRA plane perimeters and THV interaction with the surrounding anatomy was determined by comparison of pre- and post-TAVR CT scans. The study was conducted in accordance with the Declaration of Helsinki.

Table 1 Baseline demographic and echocardiographic characteristics

Baseline demographic and echocardiographic characteristics (total = 50)	
Age (years)	80 ± 6
Male, *n* (%)	35 (70)
Arterial hypertension, *n* (%)	35 (70)
Diabetes mellitus, *n* (%)	5 (10)
COPD, *n* (%)	10 (20)
History of atrial fibrillation, *n* (%)	15 (30)
Peripheral vascular disease, *n* (%)	15 (30)
Previous PCI, *n* (%)	15 (30)
GFR on baseline <60%, *n* (%)	33 (65)
NYHA class, median (IQR)	3 (2-3)
NHYA III, *n* (%)	27 (54)
NHYA IV, *n* (%)	0 (0)
STS-Risk score, median (IQR)	4.3 (3.0-6.5)
Echocardiographic data	
Left ventricle ejection fraction (EF) (%)	49 ± 12
Aortic valve area, *n* (%)	0.77 ± 0.18
Mean aortic gradient, mmHg	47 ± 10
Low-flow low gradient, *n* (%)	8 (16)
Aortic regurgitation, *n* (%)	23 (46)
Mild-moderate, *n* (%)	8 (16)
Moderate, *n* (%)	10 (20)
Severe, *n* (%)	3 (6)

CABG, coronary artery bypass graft; COPD, chronic obstructive pulmonary disease; NYHA, New York Heart Association; PCI, percutaneous coronary intervention; STS, Society of Thoracic Surgeons.

Statistical analysis

Categorical variables were expressed as frequencies and percentages, and continuous variables as means ± standard deviations or median and interquartile ranges, depending on the presence or absence of normal

Table 2 Baseline computed tomography measurements

Baseline CT characteristics (total = 50)	
Type of bicuspid aortic valve	
1, *n* (%)	47 (94)
2, *n* (%)	3 (6)
Raphe/fusion between cusps	
Between right and left, *n* (%)	34 (68)
Between right and non-coronary, *n* (%)	14 (28)
Between left and non-coronary, *n* (%)	2 (4)
Raphe characteristics	
Fibrotic raphe, *n* (%)	6 (12)
Calcific raphe, *n* (%)	44 (88)
Raphe length, mm	11.5 ± 2.4
Calcium raphe length, mm	7.2 ± 4
VBR sizing	
D_{min}, mean ± SD, mm	23 ± 3.5
D_{max}, mean ± SD, mm	28.1 ± 2.9
Perimeter, mean ± SD, mm	81.4 ± 7.1
Perimeter-derived diameter, mean ± SD, mm	26 ± 2.4
LIRA plane sizing	
Perimeter, mean ± SD, mm	73 ± 7.9
Perimeter-derived diameter, mean ± SD, mm	23.2 ± 2.5
ICD, mean ± SD, mm	26.8 ± 3.4
Height LIRA plane-VBR plane, mean ± SD, mm	7.1 ± 1.4
4 mm above VBR sizing	
Two commissures visibles, *n* (%)	19 (38%)
ICD when 2 commissures visibles, mean ± SD, mm	27.3 ± 3.3
Calcium in LVOT, *n* (%)	15 (30%)
Sinotubular junction, mean ± SD, mm	30.6 ± 3.4
Ascending aorta, major diameter	38.3 ± 4.5
Horizontal aorta, *n* (%)	11 (22%)
Coronary artery height, mm	
LMCA, mean ± SD, mm	13.6 ± 2.5
RCA, mean ± SD, mm	16.4 ± 3.8

ICD, intercommissural distance; LIRA, Level of Implantation at the RAphe; LMCA, left main coronary artery; LVOT, left ventricular outflow tract; RCA, right coronary artery; SD, standard deviation; VBR, virtual basal ring.

distribution. A paired *t*-test was used to test for differences in means with continuous variables, and a two-sided *P*-value <0.05 was considered statistically significant. The correlation of measurements was analysed using the Pearson correlation coefficient. Statistical analysis was performed using IBM SPSS Statistics version 22.0 (IBM Corporation, New York, NY, USA).

Results

A total of 50 patients were included between November 2018 and October 2021. Mean age was 80 ± 6 years and 70% were male, with a median Society of Thoracic Surgeons (STS) predicted risk of mortality score of 4.3 (3.0-6.5). Baseline characteristics of the included cohort are reported in *Table 1*. Computed tomography scans identified three different BAV anatomies: 41 patients with Type 1 BAV and a calcific raphe, 6 with Type 1 BAV and a fibrotic raphe, and 3 with Type 2 BAV. The VBR perimeter was significantly larger than the LIRA plane perimeter (81.4 ± 7.1 vs. 73 ± 7.9 mm, $P < 0.001$), confirming the typical tapered ('volcano') aortic root configuration of BAV anatomy. Two commissures were visible at a point 4 mm above the VBR in 38% of cases. Baseline CT scan measurements are reported in *Table 2* and confirm high interobserver reproducibility of LIRA plane perimeter measurements ($r = 0.980$; $P < 0.001$) (*Figure 2*).

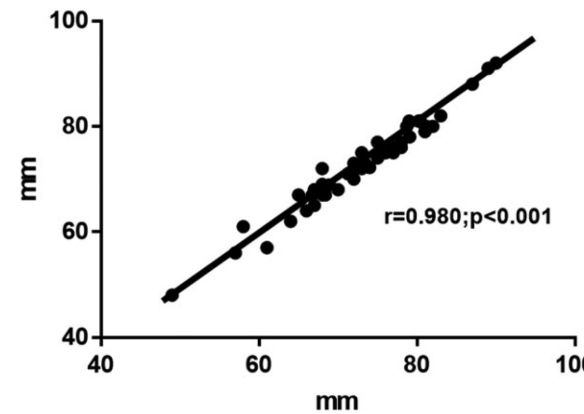

Figure 2 Interobserver correlation of the perimeter at the LIRA plane. LIRA, Level of Implantation at the RAphe.

Procedural characteristics

Transcatheter aortic valve replacement was performed under conscious sedation and THVs implanted via transfemoral access. Various supra-annular self-expandable THVs were implanted [ACURATE Neo and Neo 2 (Boston Scientific, Marlborough, MA, USA) 56%; Evolut R/Pro (Medtronic, Minneapolis, MN, USA) 44%]. Discrepancies between VBR and LIRA perimeters would have led to different valve size selection in most cases, with LIRA sizing leading to selection of a THV one size smaller in comparison with conventional annular tracing (*Figure 3A and B*). The THV was therefore sized according to manufacturer recommendations based on the LIRA plane perimeter (diameter prosthesis implanted/diameter prosthesis according to LIRA plane = 1) (DPI/DP LIRA = 1) and significantly downsized according to the VBR perimeter (DPI/DP VBR 0.89; $P < 0.001$). The median prosthesis size was 26 mm (range 23-27 mm). The need for pre-dilatation was relatively high (88%) with a median balloon size of 20 mm (range 20–23 mm), whereas post-dilatation was applied in 26% of cases (median balloon size 23 mm, range 22–24 mm). Procedural characteristics of the overall population are reported in *Table 3*—VARC-2 device success was 100% in the overall population with no valve migration, procedural mortality, cases with mean gradient >20 mmHg or moderate-severe PVL (*Table 4*).

Echocardiographic data and in-hospital and 30-day outcomes

Procedural, in-hospital, and 30-day outcomes are reported in *Table 4*. The mean THV gradient pre-discharge was 8.2 ± 3.4 mmHg—no patients had a mean gradient >20 mmHg or moderate-severe PVL. There were no strokes or mortality, and the incidence of in-hospital pacemaker implantation was 10%.

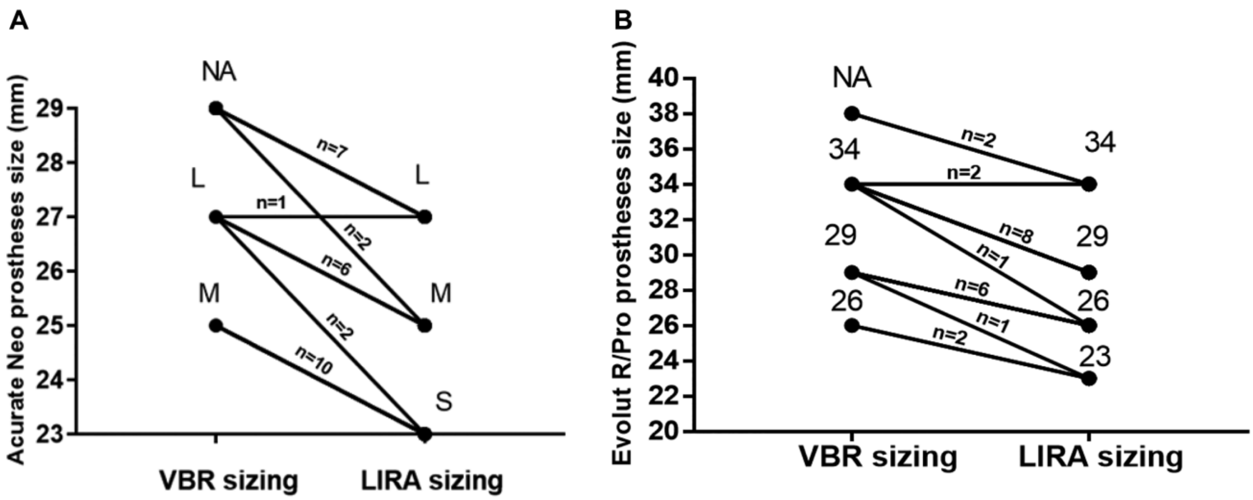

Figure 3 (*A*) Virtual basal ring and LIRA sizing of ACURATE Neo and Neo2 prostheses. (*B*) Virtual basal ring and LIRA sizing of Evolut R/Pro prostheses. NA: outside the range for specific prosthesis sizing charts and therefore not available. LIRA, Level of Implantation at the RAphe.

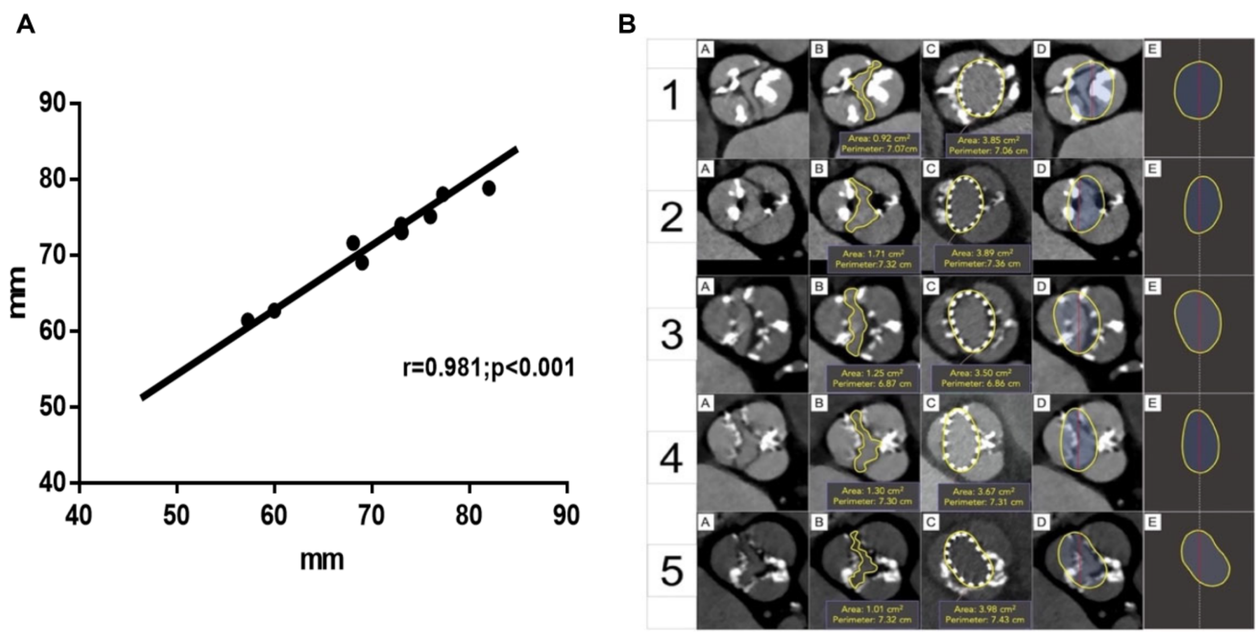

Figure 4 (*A*) Correlation between pre-transcatheter aortic valve replacement perimeter measurement at the LIRA plane and post-transcatheter aortic valve replacement prosthesis perimeter at the same level. (*B*) Prediction of the perimeter occupied by a transcatheter heart valve using CT LIRA plane sizing. Columns A and B show the LIRA plane of the bicuspid aortic valve and the perimeter traced according to the LIRA method. Column C shows the perimeter of the implanted transcatheter heart valve. Column D shows the overlap of the transcatheter heart valve perimeter on the LIRA plane, demonstrating that each valve interacts differently with the surrounding anatomy. Column E demonstrates the final shapes of the implanted valves—note significant and unpredictable variation in final ellipsoid (not elliptical) shape. LIRA, Level of Implantation at the RAphe.

Post-procedural MDCT assessment

A total of 10 post-procedural CT scans were available for analysis and demonstrated a strong correlation between the pre-TAVR LIRA plane perimeter and post-TAVR prosthesis perimeter at the same level ($r = 0.981$; $P < 0.001$) (*Figure 4A*). Transcatheter heart valve anchoring and sealing take place at the LIRA plane (mean maximal horizontal distance of 0 mm between the prosthesis cage and the leaflets), whereas at the level of the VBR there is partial interaction between the THV and the aortic annular walls (mean maximal horizontal distance of 4.5 ± 2.3 mm between the prosthesis cage and annular plane walls). The supra-annular prosthesis is elliptical at the VBR and LIRA planes, whereas a greater degree of circularity is maintained at coaptation level (mean eccentricity index 0.05 ± 0.05) (*Figure 1D-F*). The implantation level of the prosthesis was high (mean prosthesis implantation depth 3.0 ± 3.3 mm), with two cases where the ventricular edges

Table 3 Procedural characteristics

Procedural characteristics (total = 50)	
ACURATE *neo*, *n* (%)	16 (32)
S (23 mm), *n*	7
M (25 mm), *n*	4
L (27 mm), *n*	5
ACURATE *neo 2*, *n* (%)	12 (24)
S (23 mm), *n*	5
M (25 mm), *n*	4
L (27 mm), *n*	3
Evolut Pro R and Pro, *n* (%)	22 (44)
23 mm, *n*	3
26 mm, *n*	7
29 mm, *n*	7
34 mm, *n*	5
Median prosthesis size, (IQR)	26 (23-27)
Cover index	
VBR plane, median (IQR)	−4 (−5.9; −2.5)
LIRA plane, median (IQR)	5 (5.5-11.9)
Prosthesis diameter/prosthesis diameter according to VBR	0.89 ± 0.05
Prosthesis diameter/prosthesis diameter according to LIRA	1
Prosthesis diameter/prosthesis diameter according to ICD 4 mm above VBR	0.88 ± 0.03
Median prosthesis size, (IQR)	26 (23-27)
Prosthesis diameter/prosthesis diameter according to VBR	0.89 ± 0.05
Prosthesis diameter/prosthesis diameter according to LIRA	1
Prosthesis diameter/prosthesis diameter according to ICD 4 mm above VBR	0.88 ± 0.03
Pre-dilatation, *n* (%)	44 (88)
Size, mm, median (IQR)	20 (20-23)
Post-dilatation, *n* (%)	13 (26)
Size, mm, median (IQR)	23 (22-24)

IQR, interquartile range; LIRA, Level of Implantation at the RAphe; THV, transcatheter heart valve; VARC-2, Valve Academic Research Consortium-2; VBR, virtual basal ring.

Table 4 Procedural, in-hospital, and 30-day outcomes

Procedural outcome	
VARC-2 DEVICE SUCCESS	50 (100%)
Mean gradient >20 mmHg post-procedure, *n* (%)	0 (0%)
Moderate-severe PVL, *n* (%)	0 (0%)
Procedural death, *n* (%)	0 (0%)
Second valve used, *n* (%)	0 (0%)
In-hospital outcomes	
Mean gradient >20 mmHg, *n* (%)	0 (0%)
Mean gradient, mmHg, *n* ± SD	8.2 ± 3.4
Moderate-severe PVL, *n* (%)	0 (0%)
In-hospital mortality	0 (0%)
Need of permanent pacemaker, *n* (%)	5 (10%)
Stroke	0 (0%)
Discharge-30-day outcome	
Mean gradient >20 mmHg, *n* (%)	0
Moderate-severe PVL, *n* (%)	0
Mortality	0
Need of permanent pacemaker, *n* (%)	0
Stroke	0

of the prostheses frames were higher than VBR levels. Interactions between THV prostheses and the aortic root in bicuspid anatomy with raphe are reported in *Table 5*.

Discussion

Our study demonstrates that (i) supra-annular self-expandable THV sizing using the LIRA method is safe with a high device success rate in a cohort of 50 patients with raphe-type BAV disease, (ii) the aortic root generally has a tapered ('volcano') configuration in raphe-type BAV disease and LIRA sizing mostly leads to selection of a THV one size smaller compared to traditional annular tracing, (iii) LIRA plane perimeter measurement is highly reproducible, (iv) two commissures are not always visible at a point 4 mm above the VBR (< 38% of cases), (v) the LIRA plane perimeter determined from a pre-procedural CT scans can predict the perimeter occupied by the supra-annular self-expandable THV, (vi) supra-annular self-expandable prostheses maintain adequate circularity at coaptation level in raphe-type BAV disease.

Transcatheter aortic valve replacement in patients with raphe-type BAV stenosis poses several anatomical and technical challenges that may be associated with suboptimal procedural and clinical outcomes. Importantly, BAV anatomy has been excluded from randomized clinical trials evaluating the efficacy of TAVR in the treatment of severe aortic stenosis.[1-3] Despite the introduction of new-generation THVs, device success in this setting is limited by a higher likelihood of significant PVL with self-expanding prostheses and annular rupture with balloon-expandable prostheses.[10] These issues require tailored solutions as TAVR indications expand to younger patients with lower surgical risk, and a higher prevalence of BAV anatomy.[4]

Appropriate THV sizing is essential to optimize the interaction between the prosthesis and individual patient anatomy. In particular, the narrowest portion of the aortic root in BAV patients seems to be located at the level of the raphe instead of the VBR. The consequent tapered ('volcano') configuration of the aortic root leads to discrepant measurements at the annular and supra-annular plane. Various methods of supra-annular sizing have been proposed for THV sizing in BAV disease as alternatives to conventional annular tracing.[7] Liu *et al.*[21] described a sizing method using balloon pre-dilatation based on the so-called 'waist sign'—sequential pre-dilatations were performed beginning with a smaller size until the 'waist sign' appeared with less than mild regurgitation during contrast injection. Weir-McCall *et al.*[22] used the distance between the innermost aspect of the two commissures (the intercommisural distance, ICD) as the diameter of a circle to calculate perimeter and area. Alternatively, the ICD at a point 4 mm above the VBR may be used as the standardized supra-annular measurement, based upon the fact that the device landing zone usually lies 4 mm below the aortic annulus in patients with a

Table 5 Interaction between THV prostheses and the aortic root in bicuspid anatomy with raphe

	Pre-TAVI CT scan LIRA plane perimeter (mm)	Post-TAVI CT scan prosthesis perimeter at the LIRA plane (mm)	Eccentricity index THV at VBR	Eccentricity index THV at LIRA	Eccentricity index THV at coaptation level	Horizontal distance THV-leaflets at the LIRA plane (mm)	Horizontal distance THV-VBR walls (mm)	Depth of THV implantation (mm)
PT-001	68.5	71.2	0.430	0.403	0.034	0	HI	−3.3
PT-002	66.9	69.7	0.381	0.332	0.016	0	4.4	3.4
PT-003	73.1	73	0.450	0.382	0.019	0	HI	−2.2
PT-004	71.6	70.7	0.216	0.231	0.145	0	7.2	3.8
PT-005	82	78.8	0.130	0.151	0.013	0	6.3	6.6
PT-006	57.3	61.4	0.073	0.168	0.047	0	5.5	2.5
PT-007	60	62.7	0.061	0.127	0.031	0	1.1	6.5
PT-008	68.1	71.6	0.280	0.275	0.153	0	2.2	4.2
PT-009	76	75.1	0.137	0.227	0.003	0	2.7	4.6
PT-010	77.3	78	0.265	0.118	0.007	0	6.8	4.1

HI, high implantation (above VBR); THV, transcatheter heart valve; VBR, virtual basal ring.

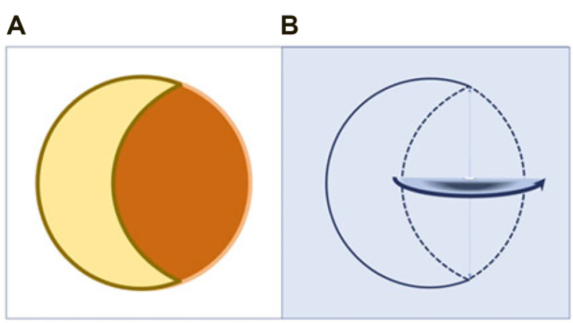

Figure 5 Geometrical assumptions underpinning the LIRA method. LIRA, Level of Implantation at the RAphe.

tri-leaflet aortic valve.[17] As an analogy, the landing zone in BAV patients could theoretically lie 4 mm above the aortic annulus given the location of the constraint points. The size of the prosthesis was therefore chosen based on the minimum value between the mean perimeter-derived diameter of the annulus and the ICD 4 mm above the VBR—according to these measurements, annulus-based sizing was applicable in 88% of patients. Furthermore, Petronio *et al.*[23] proposed the CASPER algorithm for prosthesis sizing that takes account of both the annular and supra-annular plane—starting from the annulus-derived diameter, several millimetres (up to 2.5) are subtracted to take account of the presence of heavy calcium burden, raphe length, and calcium distribution. We recently identified a supra-annular plane at raphe-level that predicts THV anchoring in raphe-type BAV disease—the LIRA (Level of Implantation at the RAphe) plane.[12] Delineation of the internal border of the leaflets (excluding all other structures encountered at this level—fused commissures, heavy calcification, and calcific or fibrotic raphes) allows derivation of the perimeter at this plane (*Figure 1B and C*) and THV sizing with optimal procedural outcome.[13] Importantly, none of these methods of supra-annular sizing have been applied in case series exceeding 20 patients. This study, therefore, represents the first substantial real-world experience using a supra-annular sizing method (the LIRA sizing method) in the anatomical setting of raphe-type BAV disease.

The LIRA plane represents a 'neo-VBR' where the perimeter delineates the internal border of the leaflets and excludes all other structures at this level. The methodology is based upon geometrical assumptions and is highly reproducible, allowing prediction of the perimeter occupied by the THV. In the anatomical setting of the elliptical BAV orifice, the perimeter is a measurable and constant value, whereas the area varies significantly throughout the cardiac cycle. This geometrical paradox may be explained by the isoperimetric concept, whereby shapes with a fixed perimeter can have different areas. This concept originally arose in relation to different closed curves with the same perimeter and a solution was provided in 1838 by Jakob Steiner, a Swiss mathematician, who demonstrated that the following inequality is applicable to all closed curves in the plane of fixed perimeter:

$$\frac{A}{P^2} \leq \frac{1}{4\pi}.$$

Thus, the relation between the area and the perimeter squared is always inferior to a constant value $\frac{1}{4\pi}$. The only exception is for circular shapes where substitution of A (numerator) with πr^2 (circle area formula), and P (denominator) with $2\pi r$ (circle perimeter formula) generates the maximum achievable value.

$$\frac{A}{P^2} = \frac{\pi r^2}{4\pi^2 r^2} = \frac{1}{4\pi}.$$

Therefore, among all closed curves in the plane of fixed perimeter, the one with the largest area is the circle (the so-called 'Steiner symmetrization').[24] *Figure 5* illustrates the geometrical assumptions underpinning the LIRA tracing method. In the left-hand panel, a lunar eclipse is shown, where the moon is superimposed upon the sun. The moon and sun are two figures with different shapes and areas but the same perimeter. However, if we turn the small curve of the moon by 180° (right-hand panel), we have two identical

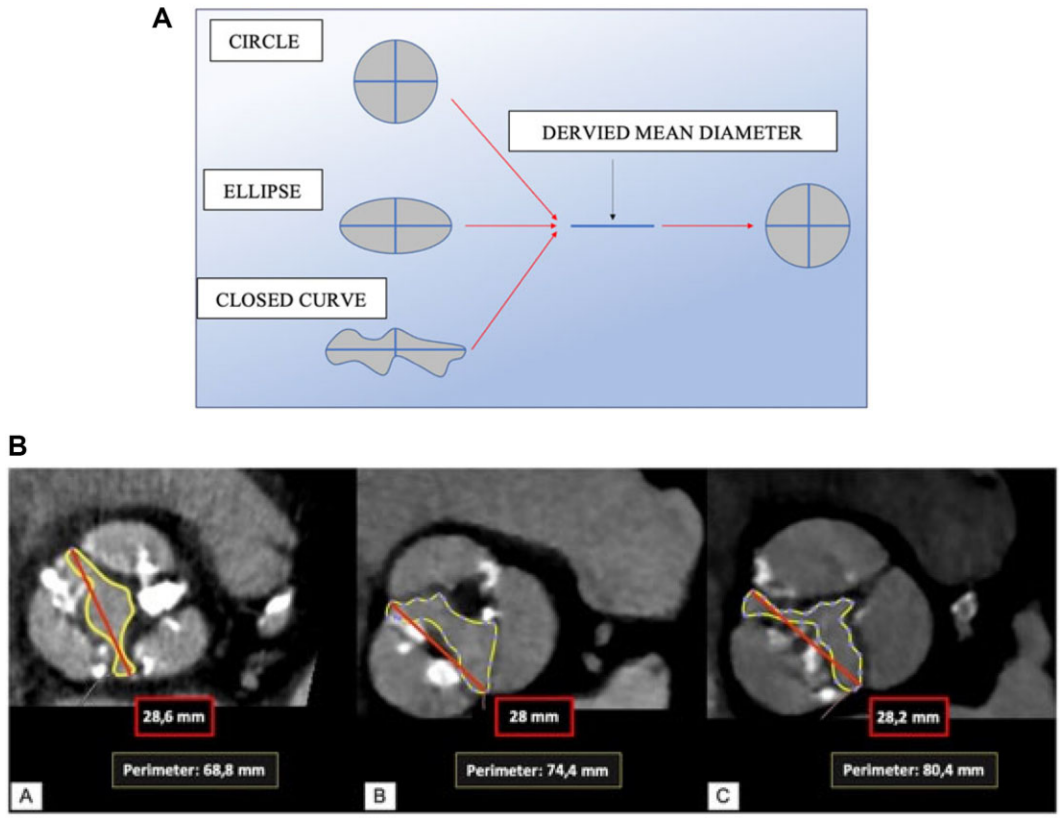

Figure 6 (*A*) Direct and inverse derivation of the mean diameter from different closed curves. (*B*) Inter-commissural distance and perimeter at the LIRA plane. (*A-C*) Three different patients with similar inter-commissural distances but different perimeters at the LIRA plane. ICD, intercommissural distance; LIRA, Level of Implantation at the RAphe.

figures. This is equivalent to the perimeter traced according to the LIRA method and the perimeter of the implanted THV—two different figures with different areas but the same perimeter. *Figure 4A and B* and *Table 5* demonstrate that the perimeter derived using the LIRA method can accurately predict the actual space occupied by the THV—in Columns B and C, the device perimeter following implantation is almost identical to the LIRA plane perimeter derived from the pre-procedural CT scan. Furthermore, Columns C and D emphasize the difficulty of predicting the final THV shape (e.g. circular[22] or hypothetical ellipse) from the pre-procedural CT scan, since this depends on interaction with the surrounding individual patient anatomy (Column E). Specifically, the presence of the raphe inhibits adequate expansion of the prosthesis at this level, independent of its characteristics (fibrotic or calcific).

Supra-annular self-expanding THVs adapt to the LIRA plane perimeter space available in this anatomical setting without modifying its value, and increase the area interacting with the surrounding anatomy. The elliptical shape of the prosthesis at the VBR and LIRA plane is balanced by greater degree of circularity at coaptation level (*Table 5*, *Figure 1D-F*). Preserved symmetry of the THV leaflets at coaptation level might account for the low residual transvalvular gradient (mean gradient $<$20 mmHg) and may determine future valve durability.[25]

In this study, the perimeter of the LIRA plane was significantly smaller than that of the VBR, conferring the typical tapered ('volcano') configuration of the aortic root in raphe-type BAV disease. Consequently, implanted THVs were at least one size smaller than would have been selected according to conventional annular tracing in most cases (*Figure 3A and B*). Tchetche *et al.*[17] previously reported that the ICD 4 mm above the VBR plane provided optimal THV sizing in relation to the mean perimeter-derived annular diameter—accordingly, most aortic root configurations were 'flare' or 'tubular', leading to a traditional annular based sizing strategy in most cases. The ICD is a unidimensional measurement between commissures with inherent limitations, whereas the perimeter is bidimensional. *Figure 6A* shows that the same mean diameter can be derived from the mean of the maximal and minimal diameter of different closed curves (circle, ellipse, or irregular shaped curve). However, the inverse derivation cannot be applied since the only figure that can be derived with certainty from a mean diameter (in terms of area and perimeter) is a circle (where maximum and minimum diameter are identical). Therefore, the ICD can only derive a circle, leading to excessive area enlargement as demonstrated by the Steiner symmetrization.[24] Furthermore, *Figure 6B*shows that ICD may not correlate with perimeter-based diameters at the LIRA plane (same ICD diameter with three different perimeters and three different THV sizes). Consequently, considering the ICD as a reference of supra-annular measurement might overestimate the actual space available, leading to the misconception of a high incidence of 'flare' or 'tube' aortic root configuration in patients with BAV anatomy and risk of aortic rupture if a balloon-expandable THV is selected.

The ICD 4 mm above the VBR is based upon the fact that the landing zone is usually 4 mm below the aortic annulus in patients with a tri-leaflet aortic valve. As an analogy, the landing zone in BAV patients could theoretically run 4 mm above the aortic annulus given the location of the constraint points.[17] However, the LIRA plane cannot be arbitrarily located at a fixed distance above the VBR since its location differs in each patient.[12] In addition, measurement of ICD 4 mm above the VBR may be problematic since this plane might not be high enough to identify two commissures in Types 1 and 2 anatomy. Indeed, three commissures were visualized in 62% of our patient cohort.

In this study, we report the feasibility of LIRA sizing in 50 prospective and consecutive TAVR procedures using various supra-annular self-expanding prostheses in a range of raphe-type BAV anatomies. Pre-dilatation was performed frequently (88%) with a median balloon size of 20 mm, whereas post-dilatation was performed in only 26% of cases. We propose that this strategy of aggressive pre-dilatation (20 mm balloon) in relation to the LIRA plane (LIRA perimeter-derived diameter 23 mm) enhanced optimal expansion during THV deployment and reduced the need for post-dilatation to obtain an adequate result *Table 3*. Procedural outcomes were optimal (100% VARC-2 device success) with no valve migration, adequate prosthesis expansion, trivial/mild residual PVL, and low transprosthetic gradient, and maintained at 30 days. Furthermore, the incidence of in-hospital pacemaker implantation was low (10%), reflecting high THV implantation in relation to the level of the LIRA plane and the low prosthesis interaction with the membranous septum *Table 4* and *Table 5*.[26]

Limitations

Our study has several limitations. First, this was a single-centre non-randomized study. Second, imaging assessment for the diagnosis of BAV and evaluation of echocardiographic outcomes was not performed by a core laboratory. Third, our proposed sizing algorithm (LIRA method) requires validation in a larger prospective multicentre registry.

Conclusions

This study confirms that supra-annular sizing using the LIRA method in raphe-type BAV patients is safe in a large cohort of patients and is associated with high device success using various supra-annular self-expandable THVs. Further, larger studies are needed to confirm these findings.

Acknowledgement

This study has been awarded with the prize "Premio Vincenzo Masini" 2022 from the Italian Association of Hospital Cardiologists (ANMCO).

Funding

None.

Conflict of interest: M.M. serves as a proctor for Boston Scientific. B.P. has received unrestricted research and educational grants from Edwards Lifesciences, lecture fees from Edwards Lifesciences, Medtronic, and Abbott, and consultancy fees from Anteris and Microport. The other authors have nothing to disclose.

Data availability

The data underlying this article are available in the article and in its online supplementary material.

References

1. Makkar RR, Fontana GP, Jilaihawi H, Kapadia S, Pichard AD, Douglas PS, Thourani VH, Babaliaros VC, Webb JG, Herrmann HC, Bavaria JE, Kodali S, Brown DL, Bowers B, Dewey TM, Svensson LG, Tuzcu M, Moses JW, Williams MR, Siegel RJ, Akin JJ, Anderson WN, Pocock S, Smith CR, Leon MB; PARTNER Trial Investigators. Transcatheter aortic-valve replacement for inoperable severe aortic stenosis. *N Engl J Med* 2012;**366**:1696–1704.
2. Leon MB, Smith CR, Mack MJ, Makkar RR, Svensson LG, Kodali SK, Thourani VH, Tuzcu EM, Miller DC, Herrmann HC, Doshi D, Cohen DJ, Pichard AD, Kapadia S, Dewey T, Babaliaros V, Szeto WY, Williams MR, Kereiakes D, Zajarias A, Greason KL, Whisenant BK, Hodson RW, Moses JW, Trento A, Brown DL, Fearon WF, Pibarot P, Hahn RT, Jaber WA, Anderson WN, Alu MC, Webb JG; PARTNER 2 Investigators. Transcatheter or surgical aortic-valve replacement in intermediate-risk patients. *N Engl J Med* 2016;**374**:1609–1620.
3. Mack MJ, Leon MB, Thourani VH, Makkar R, Kodali SK, Russo M, Kapadia SR, Malaisrie SC, Cohen DJ, Pibarot P, Leipsic J, Hahn RT, Blanke P, Williams MR, McCabe JM, Brown DL, Babaliaros V, Goldman S, Szeto WY, Genereux P, Pershad A, Pocock SJ, Alu MC, Webb JG; PARTNER 3 Investigators. Transcatheter aortic-valve replacement with a balloon-expandable valve in low-risk patients. *N Engl J Med* 2019;**380**:1695–1705.
4. Tutar E, Ekici F, Atalay S, Nacar N. The prevalence of bicuspid aortic valve in newborns by echocardiographic screening. *Am Heart J* 2005;**150**:513–515.
5. Ward C. Clinical significance of the bicuspid aortic valve. *Heart* 2000;**83**:81–85.
6. Roberts WC, Ko JM. Frequency by decades of unicuspid, bicuspid, and tricuspid aortic valves in adults having isolated aortic valve replacement for aortic stenosis, with or without associated aortic regurgitation. *Circulation* 2005;**111**:920–925.
7. Costa G, Angelillis M, Petronio AS. Bicuspid valve sizing for transcatheter aortic valve implantation: the missing link. *Front Cardiovasc Med* 2022;**8**:1–7.
8. Yoon SH, Lefèvre T, Ahn JM, Perlman GY, Dvir D, Latib A, Barbanti M, Deuschl F, De Backer O, Blanke P. Transcatheter aortic valve replacement with early- and new-generation devices in bicuspid aortic valve stenosis. *J Am Coll Cardiol* 2016;**68**:1195–1205.
9. Perlman GY, Blanke P, Dvir D, Pache G, Modine T, Barbanti M, Holy EW, Treede H, Ruile P, Neumann FJ. Bicuspid aortic valve stenosis: favorable early outcomes with a next-generation transcatheter heart valve in a multicenter study. *JACC Cardiovasc Interv* 2016;**9**:817–824.
10. Montalto C, Sticchi A, Crimi G, Laricchia A, Khokhar AA, Giannini F, Reimers B, Colombo A, Latib A, Waksman R, Mangieri A. Transcatheter aortic valve replacement in bicuspid versus tricuspid anatomy. *JACC Cardiovasc Interv* 2021;**14**:2144–2155.
11. Yoon SH, Kim WK, Dhoble A, Milhorini Pio S, Babaliaros V, Jilaihawi H, Pilgrim T, De Backer O, Bleiziffer S, Vincent F, Shmidt T, Butter C, Kamioka N. Bicuspid aortic valve morphology and outcomes after transcatheter aortic valve replacement. *J Am Coll Cardiol* 2020;**76**:1018–1030.

12. Iannopollo G, Romano V, Buzzatti N, De Backer O, Søndergaard L, Merkely B, Prendergast BD, Giannini F, Colombo A, Latib A, Granada JF, Chieffo A, Montorfano M. A novel supra-annular plane to predict TAVI prosthesis anchoring in raphe-type bicuspid aortic valve disease: the LIRA plane. *Eurointervention* 2020;**16**:259–261.
13. Iannopollo G, Romano V, Buzzatti N, Ancona M, Ferri L, Russo F, Bellini B, Granada JF, Chieffo A, Montorfano M. Supra-annular sizing of transcatheter aortic valve prostheses in raphe-type bicuspid aortic valve disease: the LIRA method. *Int J Cardiol* 2020;**317**:144–151.
14. Sievers HH, Schmidtke C. A classification system for the bicuspid aortic valve from 304 surgical specimens. *J Thorac Cardiovasc Surg* 2007;**133**:1226–1233.
15. Vahanian A, Beyersdorf F, Praz F, Milojevic M, Baldus S, Bauersachs J, Capodanno D, Conradi L, De Bonis M, De Paulis R, Delgado V, Freemantle N, Gilard M, Haugaa KH, Jeppsson A, Jüni P, Pierard L, Prendergast BD, Sádaba JR; ESC/EACTS Scientific Document Group. 2021 ESC/EACTS Guidelines for the management of valvular heart disease: developed by the task force for the management of valvular heart disease of the European Society of Cardiology (ESC) and the European Association for Cardio-Thoracic Surgery (EACTS). *Eur Heart J* 2022;**43**:561–632.
16. Kim WK, Möllmann H, Liebetrau C, Renker M, Rolf A, Simon P, Van Linden A, Arsalan M, Doss M, Hamm CW, Walther T. The ACURATE Neo transcatheter heart valve: a comprehensive analysis of predictors of procedural outcome. *JACC Cardiovasc Interv* 2018;**11**: 1721–1729.
17. Tchetche D, de Biase C, van Gils L, Parma R, Ochala A, Lefevre T, Hovasse T, De Backer O, Sondergaard L, Bleiziffer S, Lange R, Kornowski R, Landes U, Norgaard BL, Biasco L, Philippart R, Molina-Martin de Nicolas J, Mylotte D, Lemee C, Dumonteil N, Van Mieghem NM. Bicuspid aortic valve anatomy and relationship with devices: the BAVARD multicenter registry. *Circ Cardiovasc Interv* 2019;**12**:1–10.
18. Wong DTL, Bertaso AG, Liew GYH, Thomson VS, Cunnington MS, Richardson JD et al. Relationship of aortic annular eccentricity and paravalvular regurgitation post transcatheter aortic valve implantation with CoreValve. *J Invasive Cardiol* 2013;**25**:190–195.
19. Breitbart P, Minners J, Hein M, Schröfel H, Neumann FJ, Ruile P. Implantation depth and its influence on complications after TAVI with self-expanding valves. *Int J Cardiovasc Imaging* 2021;**37**: 3081–3092.
20. Pibarot P, Hahn RT, Weissman NJ, Monaghan MJ. Assessment of paravalvular regurgitation following TAVR: a proposal of unifying grading scheme. *JACC Cardiovasc Imaging* 2015;**8**:340–360.
21. Liu X, He Y, Zhu Q, Gao F, He WYL. Supra-annular structure assessment for self-expanding transcatheter heart valve size selection in patients with bicuspid aortic valve. *Catheter Cardiovasc Interv* 2018; **91**:986–994.
22. Weir-McCall JR, Attinger-Toller A, Blanke P, Perlman GY, Sellers SL, Wood D, Webb JG, Leipsic J. Annular versus supra-annular sizing for transcatheter aortic valve replacement in bicuspid aortic valve disease. *J Cardiovasc Comput Tomogr* 2020;**14**:407–413.
23. Petronio AS, Angelillis M, De Backer O, Giannini C, Costa G, Fiorina C, Castriota F, Bedogni F, Laborde JC, Søndergaard L. Bicuspid aortic valve sizing for transcatheter aortic valve implantation: development and validation of an algorithm based on multi-slice computed tomography. *J Cardiovasc Comput Tomogr* 2020;**14**:452–461.
24. Fusco N. The classical isoperimetric theorem. *Rend Dell'Accademia Delle Sci Fis e Mat Di Napoli* 2004;71.
25. Rodriguez-Gabella T, Voisine P, Puri R, Pibarot P, Rodés-Cabau J. Aortic bioprosthetic valve durability: incidence, mechanisms, predictors, and management of surgical and transcatheter valve degeneration. *J Am Coll Cardiol* 2017;**70**:1013–1028.
26. Hamdan A, Guetta V, Klempfner R, Konen E, Raanani E, Glikson M, Goitein O, Segev A, Barbash I, Fefer P, Spiegelstein D, Goldenberg I, Schwammenthal E. Inverse relationship between membranous septal length and the risk of atrioventricular block in patients undergoing transcatheter aortic valve implantation. *JACC Cardiovasc Interv* 2015;**8**:1218–1228.